
Theses and Dissertations

Spring 2009

Facilitating four-dimensional quantitative analysis of aortic MRI for clinical use

Senthil Kumar Premraj
University of Iowa

Copyright 2009 Senthil Kumar Premraj

This thesis is available at Iowa Research Online: <http://ir.uiowa.edu/etd/260>

Recommended Citation

Premraj, Senthil Kumar. "Facilitating four-dimensional quantitative analysis of aortic MRI for clinical use." MS (Master of Science) thesis, University of Iowa, 2009.
<http://ir.uiowa.edu/etd/260>.

Follow this and additional works at: <http://ir.uiowa.edu/etd>



Part of the [Electrical and Computer Engineering Commons](#)

FACILITATING FOUR-DIMENSIONAL QUANTITATIVE ANALYSIS OF
AORTIC MRI FOR CLINICAL USE

by

Senthil Kumar Premraj

A thesis submitted in partial fulfillment of the
requirements for the Master of Science degree
in Electrical and Computer Engineering
in the Graduate College of
The University of Iowa

May 2009

Thesis Supervisor: Professor Milan Sonka

Graduate College
The University of Iowa
Iowa City, Iowa

CERTIFICATE OF APPROVAL

MASTER'S THESIS

This is to certify that the Master's thesis of

Senthil Kumar Premraj

has been approved by the Examining Committee for the thesis requirement for the Master of Science degree in Electrical and Computer Engineering at the May 2009 graduation.

Thesis Committee: _____
Milan Sonka, Thesis Supervisor

Andreas Wahle

Thomas Scholz

TABLE OF CONTENTS

LIST OF TABLES	iv
LIST OF FIGURES	v
CHAPTER	
1 MEDICAL BACKGROUND	1
1.1 Marfan Syndrome	1
1.1.1 Introduction	1
1.2 Clinical Background	1
1.2.1 Anatomy of the Aorta	1
1.2.2 Marfan Aorta	1
1.2.3 MFS Patient Treatment	2
1.2.4 Current Diagnosis Method	4
2 PROJECT OVERVIEW	5
2.1 Hypothesis	5
2.2 Analysis Components	5
2.3 Current Status	6
2.4 Thesis Overview	7
3 4D DICOM SORTING	9
3.1 Introduction	9
3.2 Old Method	10
3.2.1 Algorithm	10
3.2.2 Administrative Overhead	11
3.3 New Method	11
3.3.1 User Interface	12
4 AORTIC SEGMENTATION	14
4.1 Introduction	14
4.2 Implementation	14
5 MEASUREMENT EXTRACTION	16
5.1 Introduction	16
5.2 Old Method	16
5.2.1 Problems	17
5.3 New Method	18
5.3.1 Overview	18

5.3.2	Volumetric Object Creation	19
5.3.3	Centerline Extraction	19
5.3.4	Normal Vector Calculation	20
5.3.5	Contour Points Extraction	23
5.3.6	Contour Points Ordering	24
5.3.7	Measurement Calculation	25
5.3.8	Measurement Validation	26
5.3.9	User Interface	30
6	MEASUREMENT ANALYSIS	36
6.1	Subject Information	36
6.2	Scan Analysis	37
6.2.1	Measurement Database	37
6.2.2	Feature Extraction	37
6.2.3	Feature Plots	38
7	CONCLUSION	46
7.1	Conclusion	46
7.2	Future Work	46
	REFERENCES	48

LIST OF TABLES

Table

5.1	Measurements and Errors For Each Slice Of Straight Cylindrical Phantom Of Diameter = 10mm, Interval = 2mm	29
5.2	Measurement Error For Aortic Binary Phantom With Various Diameters	29
6.1	Scan Distribution	36

LIST OF FIGURES

Figure

1.1	Anatomy of the Aorta	2
1.2	An illustration showing the three layers in the aorta. The Media is responsible for the aorta's elastic properties [1]	3
1.3	Aortic Aneurysms	3
2.1	Project Flow Chart.	6
3.1	Illustration of the old method of DICOM image alignment using a fixed time threshold - A fixed interval from the time stamps of the first slice are used to sort the images by phase as shown via the blue lines. 1 - A slice from phase 2 is added to phase 1, 2 - An example of a certain slice position missing a phase image since there were no images that belonged in the time interval.	10
3.2	DICOM Sorter Program.	12
4.1	Four-Dimensional Segmentation Application.	15
5.1	Cross Sectional Area (CSA) measurements in mm^2 across the length of the aorta in a normal subject for a single phase obtained using the old method. Note - The aorta is getting bigger near the diaphragm does not correlate with clinical knowledge	18
5.2	Aortic Volume Creation - Effect of Smoothing Parameter. A - No Smoothing, B - 0.1, C - 0.01, D - 0.0001	20
5.3	Aortic volume scaled to real world coordinates and centerline in image coordinates. The image is scaled and translated in 3D with respect to the centerline but the 2D graphic does not show it clearly.	21
5.4	Aortic Volume along with the centerline.	22
5.5	Aortic volume along with the cross section planes used to extract the contour points. Left - non smoothed planes, Right - Smoothed Planes.	23
5.6	volumetric cubes connecting the contour points of the aorta. Left - 10 contour points per slice connected through the whole aorta. Right - 100 contour points for a single slice.	25
5.7	Straight Phantom Cylinder Created in Floating Point Space. Diameter = 10mm, Interval = 2mm.	28

5.8	Binary Phantom of 40mm diameter along with the contour points shown as splines. Note the centerline extraction error near the diaphragm area fixed the smoothing of normals.	30
5.9	Diameter of the Binary Phantom.	31
5.10	Aortic Analysis Viewer.	32
6.1	Max CSA distribution between normal subjects and patients	40
6.2	Max CSA for patient with 5 consecutive scans	41
6.3	Patient with distal dialation in sequential scans	41
6.4	Pre and post Surgery CSA	42
6.5	Centroid Movement plot between normals and patients	42
6.6	Centroid Movement Scan for a patient with sequential scans	43
6.7	Distensiblity distribution between normal subjects and patients	43
6.8	Distensiblity distribution between normal subjects and patients	44
6.9	Curvature distribution between normal subjects and patients	44
6.10	Curvature Change between normal subjects and patients	45
6.11	Eccentricity between normal subjects and patients	45

CHAPTER 1 MEDICAL BACKGROUND

1.1 Marfan Syndrome

1.1.1 Introduction

Marfan Syndrome (MFS) is a systemic disorder of the connective tissue that affects about 1 in 5000 people in this world. It is estimated that about 60,000 to 200,000 people are affected by MFS in the US [2].

MFS affects the skeletal system, eyes, lungs and nervous system. However, one of the most serious conditions associated with MFS involves the cardiovascular system. The most serious sign is a dilated aorta as this would increase likelihood of aortic rupture and subsequent death of the patient [3] within a few hours.

1.2 Clinical Background

1.2.1 Anatomy of the Aorta

The aorta is the largest vessel in the body that transfers oxygenated blood from the heart to the rest of the body. It begins at the aortic valve located at the end of the left ventricular outflow tract. On average this vessel has a diameter of three centimeters when it leaves the ventricle and decreases to an average size of one and three-fourth centimeters at the junction of the left and right iliac arteries located in the pelvic region. MFS patients are mainly affected in the upper region of the aorta known as the thoracic aorta. Some of the major parts of the thoracic aorta are shown in Figure 1.1 on page 2.

1.2.2 Marfan Aorta

The main reason for aortic dilation in MFS patients is the degradation of connective tissue in the aorta. Connective tissues are glue-like substances holding the various parts of our body together. In the case of the aorta, the connective tissue is in the middle layer of the aortic wall known as media as shown in Figure 1.2 on

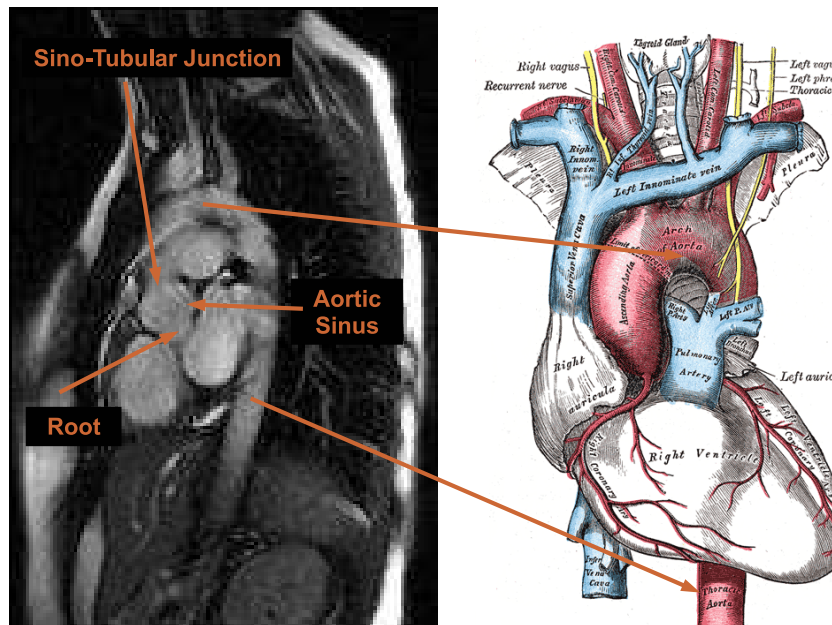


Figure 1.1: Anatomy of the Aorta [4] [5].

page 3. The media degrades in MFS patients and causes the aorta to lose its elastic properties [1]. Continuous pumping of blood into the weakened aorta by the heart causes the dilation of the aorta and eventual rupture. An illustration of the various forms of dilation in the thoracic aorta is shown in Figure 1.3 on page 3.

1.2.3 MFS Patient Treatment

There is no cure for MFS but the life expectancy has significantly increased to an age of approximately 74 years for women and 70 years for men [3] through preventative medication. The patient goes through regular heart checkups to monitor their heart valves and dilation of the aorta. Aortic dilation is kept under control by reducing the heart rate and blood pressure of the patient [3]. If the size of the aorta progresses to a significant diameter (5 cm) then surgery is necessary [3].

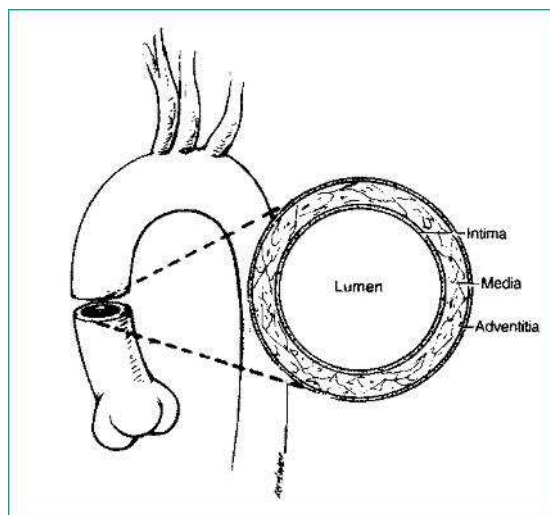


Figure 1.2: An illustration showing the three layers in the aorta. The Media is responsible for the aorta's elastic properties [1]

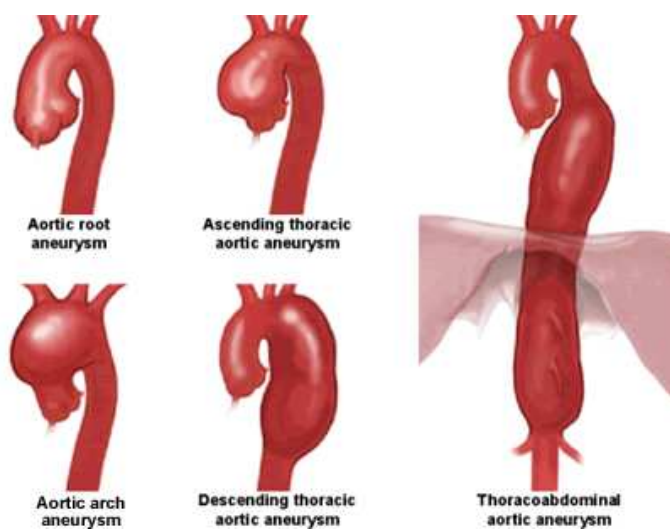


Figure 1.3: Aortic Aneurysms [4] [6].

1.2.4 Current Diagnosis Method

As explained above, constant monitoring is an essential part of the treatment plan for the patient. The most common method for monitoring is through echocardiogram using the ultrasound imaging modality.

Currently MFS aortas are monitored using two-dimensional measurements prescribed by Roman et al. [7]. However, this suffers from two shortcomings, they are:

1. Only the measurements near the aortic root are used for monitoring the patients. Hence, the dilation in the distal regions of the aorta is not monitored.
2. Measurements are manually extracted from a two-dimensional interface. Hence, it is prone to inter- and intra-observer variability.

With recent advances in cardiac MRI imaging, three-dimensional images of the aorta across the entire cardiac cycle can be obtained. However, the methodology to fully utilize this information clinically has not been developed.

CHAPTER 2 PROJECT OVERVIEW

2.1 Hypothesis

The aim of the project is to develop a methodology to utilize the three-dimensional and four-dimensional information available in cardiac MRI. It contains two hypothesis specifically:

1. Understanding the measurements across the entire length of the aorta will provide more insight into disease progression. Especially allowing the analysis of aortic dilation in the distal regions of the vessel.
2. Analyzing the motion properties will allow us to identify disease earlier since the motion of the aorta changes as the media degrades.

2.2 Analysis Components

To test the following hypothesis, various tools need to be developed. The complete analysis consists of the following components. An illustration of the project flow is given in Figure 2.1 on page 6.

1. Candy Cane (CC) and Left Ventricular Outflow Tract (LVOT) CINE acquisitions are performed using a cardiac gated sequence in a MRI scanner.
2. The information from the CC and LVOT images are combined for automatic segmentation of the aorta.
3. The aorta is segmented from the MRI images.
4. Contours are analyzed at multiple locations in the aorta to extract measurements from them.
5. Geometrical measurements about the shape and size of the aorta are calculated from the contours.

6. Measurements are analyzed to test the above hypothesis.
7. Advanced analysis using pattern recognition is also performed using the measurements and contour points.

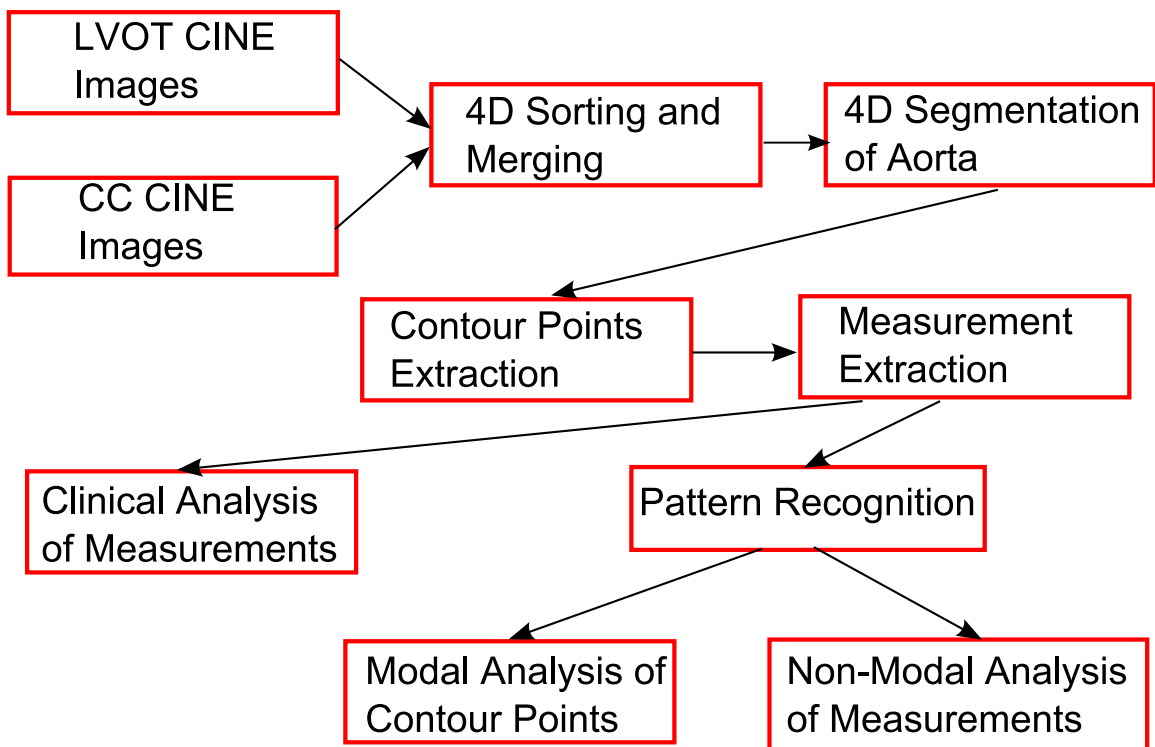


Figure 2.1: Project Flow Chart.

2.3 Current Status

1. A methodology to sort and merge the information from LVOT and CC CINE images for automatic segmentation of the aorta was developed by Andreas Wahle and Honghai Zhang. The merging algorithm was performing well but sorting the DICOM images was problematic. More information on this is provided in Chapter 3.

2. An algorithm to segment the aorta based on minimal user input was developed by Fei Zhao. While this algorithm was robust for a wide dataset, it was not usable by a clinician due to the lack of an application interface. Also, there were segmentation errors in some cases but the tool for editing the segmentation results was not robust. More information on this is provided in Chapter 4 and Chapter 5
3. A methodology to extract measurements from the segmentation result was performed by Matt Thomas. The measurements produced by this methodology did not correlate with the clinical knowledge. Hence a detailed inspection of this methodology was needed. More information on this is provided in Chapter 5

2.4 Thesis Overview

The aim of my thesis is to identify the problems in the existing methodologies and provide solutions to extract four-dimensional quantitative measurements from LVOT and CC CINE images for a wide dataset normal subjects and patients. The solutions can be a combination of developing new robust methodologies and transforming the problem for easy clinician interaction. A method for combining the various components of the project based on the existing system was also needed so there is minimal overhead for the clinician. It consisted of the following solutions:

1. An application and methodology for efficiently sorting and merging the DICOM images from the cardiac MRI scanner.
2. An application for segmenting the aorta using the existing segmentation algorithm.
3. An application and methodology to validate and correct the segmented aorta and extract quantitative measurements from the segmented aorta.

4. Analysis of the quantitative measurements extracted from both normal subjects and patients to experiment its usefulness and robustness.

CHAPTER 3 4D DICOM SORTING

3.1 Introduction

Left Ventricular Outflow Tract (LVOT) images are used to view the aortic root and Candy Cane (CC) images are used to view the distal portions of the aorta. Information from both these images should be combined to increase the coverage from both views, obtain their geometric correspondence and interpolate the voxels to an isotropic volume in order to perform automatic segmentation of the aorta. This merging of CC and LVOT views was performed by Honghai Zhang.

Before the images are combined, all the two-dimensional (2D) slices must be ordered into a four-dimensional (4D) sequence. While standards for multi-dimensional images exists, the industry follows DICOM standards 2D imaging parameters only. The three-dimensional (3D) and 4D sorting of the 2D images are performed using the positional information and time stamps available in the DICOM data.

3D imaging is performed for most advanced applications. Sorting the 2D images into a stack that converts to a 3D image is relatively simple using the consistent positional information available in the DICOM data. The time stamps must also be considered in 4D imaging. Ideally all the images belonging to a phase will have the same time stamp across all slice positions. However, this is not the case with a cardiac MRI for some vendors. The time stamps across all positions in a phase have a certain range of variability and the variability cannot be predicted easily as shown in Figure 3.1 on page 10.

Along with the basic acquisition data problems, there are other bureaucratic challenges. There are no standardized descriptors to identify the LVOT and CC images automatically. Some vendors might choose to use a different identifier tag during re-acquisition of a slice. Hence, automatically searching an identifier tag need not provide us with the necessary set of images for a series in all cases.

3.2 Old Method

3.2.1 Algorithm

The sorting of images was performed using a specific time interval threshold. For example, an image was added to a phase if it's time stamp is within a certain fixed interval to its neighboring slice as shown in Figure 3.1 on page 10. Then the slices were sorted by position. This was extremely problematic because the time interval was a fixed threshold and there was no guarantee that all the slices that correspond to a certain phase will fall within this threshold. There were two kind of problems that were encountered with this method.

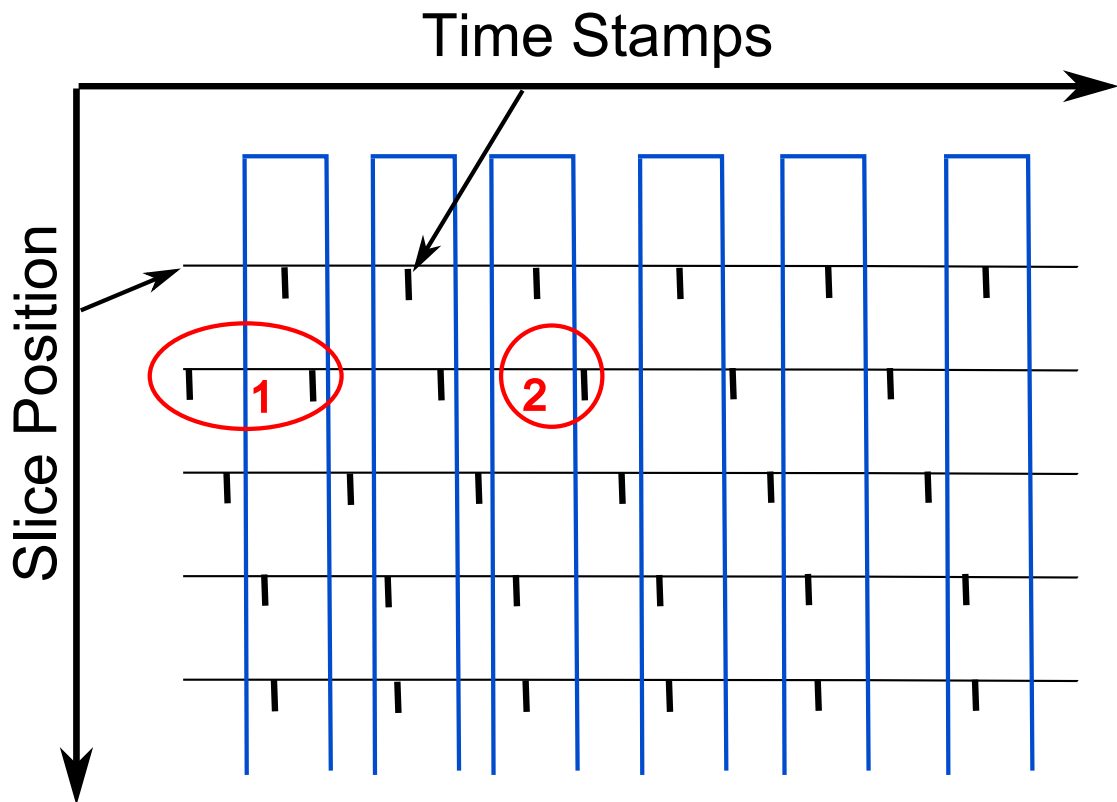


Figure 3.1: Illustration of the old method of DICOM image alignment using a fixed time threshold - A fixed interval from the time stamps of the first slice are used to sort the images by phase as shown via the blue lines. 1 - A slice from phase 2 is added to phase 1, 2 - An example of a certain slice position missing a phase image since there were no images that belonged in the time interval.

1. Certain phases can end up with an image from another phase as the time stamps may vary among slice positions. Shown in Figure 3.1 on page 10.
2. Certain phases might not have any images for a particular slice position if there were no images with time stamps in that interval. Shown in Figure 3.1 on page 10.

3.2.2 Administrative Overhead

The data management and assessment issues used before are discussed in [8]. Some XML files were used for identifying the tags that corresponded to the LVOT CINE and CC CINE images. Each series was identified using the series description available in the DICOM data. It was further validated using some open source MRI viewing programs such as MRICro.

A similar process was used to evaluate the sorting of 4D images. Any errors in sorting were corrected by editing the XML file. These processes were time consuming and could only be performed by a trained engineer. Hence a Graphical User Interface (GUI) application was needed that will combine the time consuming task of identifying the necessary tags and evaluating the sorting accuracy of the algorithm.

3.3 New Method

The new method of sorting the 2D images was performed in the following fashion:

1. All the 2D DICOM images in a series were grouped based on their acquisition geometry.
2. The groups were sorted based on their geometry.
3. The images in each group were sorted in ascending order based on the time stamps available in their DICOM data.

The GDCM library available in the ITK toolkit was used for reading the DICOM images. The grouping of the images was robust as the DICOM images had consistent

positional information. The absolute values of time stamps are not consistent across slice positions but their ordering is, hence the above sorting method would work well.

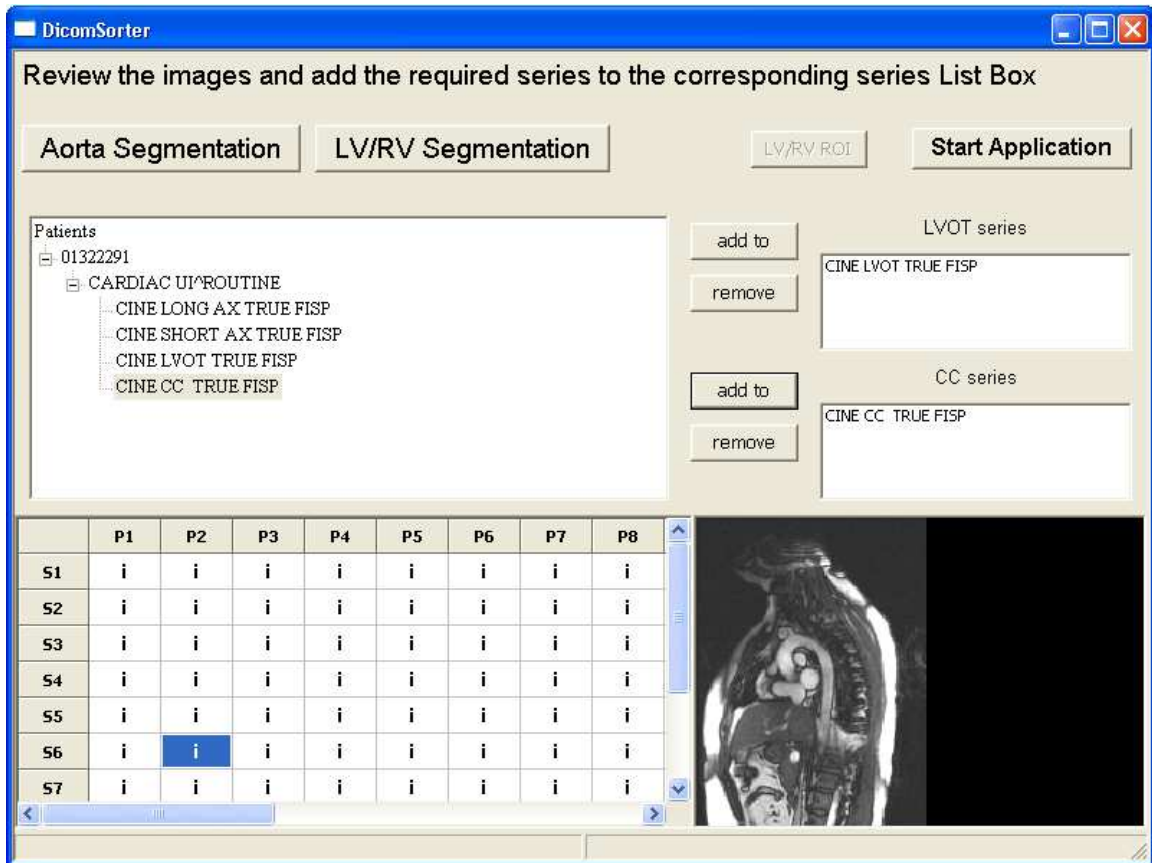


Figure 3.2: DICOM Sorter Program.

3.3.1 User Interface

The above methodology only solves the problem of sorting the necessary slices of a specific series. However, most MRI acquisitions contain multiple series of images marked by the series description. Matching the series description to LVOT or CC CINE images can only be performed by a manual observer. Sometimes the same series

can also be marked as multiple series ID by the manufacturer. Also, re-acquisition of a slice can have the same identifier or different identifier. An easy to use GUI was needed to identify these variations and solve them.

The user interface was built using the wxWidgets GUI toolkit as shown in Figure 3.2 on page 12. The interface has the following work flow:

1. Load all the images and group them by their Series ID and display the series description of each series ID in the interface.
2. The user selects a series and all images within that series are sorted as described above and shown in a grid.
3. Selecting the items on the grid displays its corresponding image. The user can validate the ordering of the images in terms of slice position and phase using this feature.
4. Sometimes certain slice locations are re-acquired so the original slice location may need to be removed from a series. The user can deselect a specific slice location by selecting its row in the grid.
5. The series can be added to the LVOT bin or CC bin accordingly after validating its slices.
6. If multiple series are used, then each of them can be validated and added to the corresponding bin.
7. The interface sorts all the image series added to the bins and merges them for segmentation.

CHAPTER 4 AORTIC SEGMENTATION

4.1 Introduction

4D Aortic segmentation was by performed Zhao et al. [9]. However, this approach is purely command line based so it is unusable by a clinician. My aim is to develop an interface to place the initial seed points, segment the aorta using the algorithms developed by Zhao et al. and display the segmentation result.

4.2 Implementation

The implementation for the GUI was built using wxWidgets toolkit. The basic image viewing capability was extracted from an existing user interface and additional functionality to place the specific seed points were developed. The input to the algorithm required three seed points and one region of interest (ROI). The first two seed points were placed in the LVOT image. One near the annulus and another at the mid-point that denotes the direction of the ascending aorta. The last seed point is to be placed in the diaphragm in the CC image to denote the end point of the segmentation. All the seed points need to be placed in the center of the aortic lumen for the algorithm to perform properly. Finally, the ROI is to be placed surrounding the aorta in the CC image.

The user interface consisted of the following features and workflow:

1. The user can view the LVOT images in all three orthogonal views and the XY plane of the CC image in the fourth viewport or vice versa. The image series (LVOT or CC) that is used as the primary set to view in all three orthogonal planes can be changed with a single button click.
2. Each seed point is placed in the necessary image in the XY plane. It can then be edited in all three orthogonal planes to center the point three-dimensionally.
3. The ROI is placed on the CC view by clicking on a location in the XY plane and

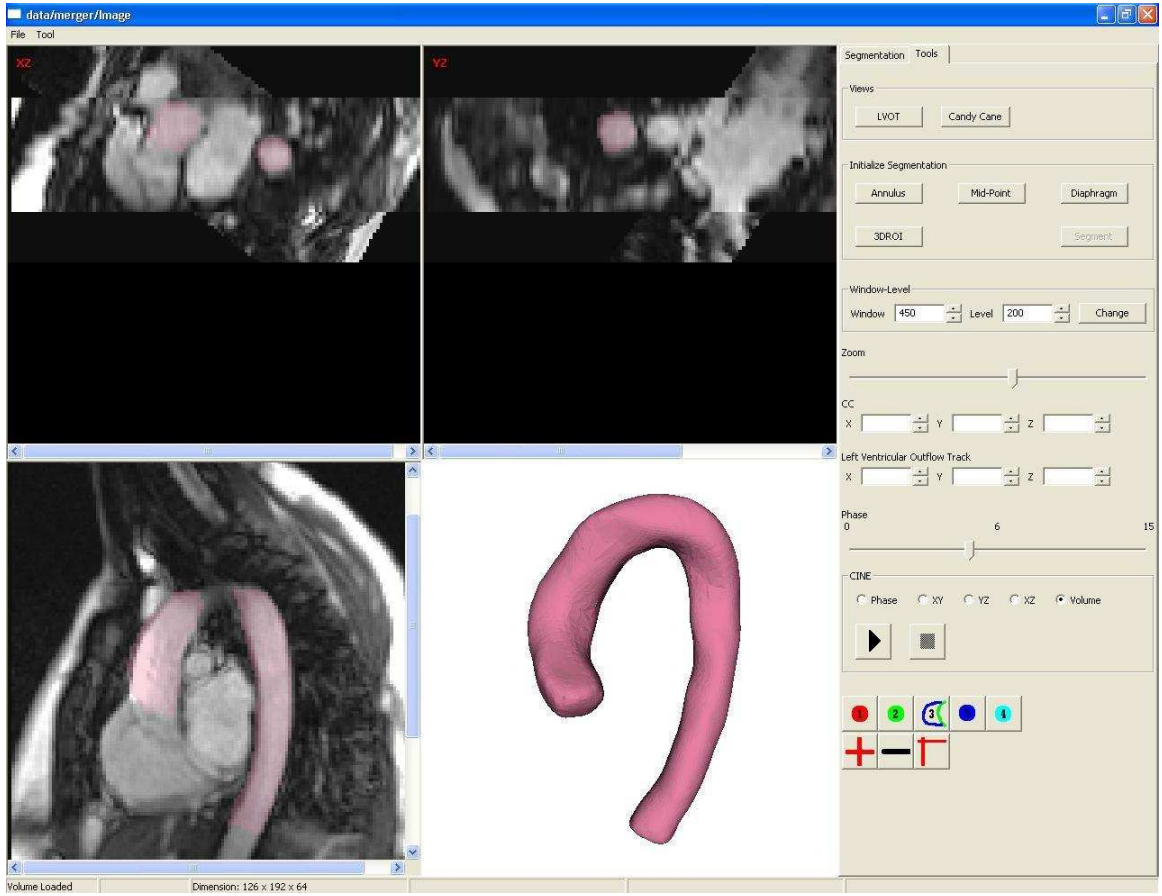


Figure 4.1: Four-Dimensional Segmentation Application.

dragging the mouse to place a rectangle. The rectangle can then be changed on all three orthogonal planes by clicking its end and dragging the mouse.

4. Then the **Segment** button is clicked to segment the aorta. The segmentation result is a binary image which represent the aortic volume. The segmentation result is displayed as an overlay on the 2D image and as a 3D view. The 3D view was displayed using the VTK toolkit integrated into wxWidgets via the *wxVTKRenderWindowInteractor* class.

CHAPTER 5 MEASUREMENT EXTRACTION

5.1 Introduction

The main purpose of the segmentation is to evaluate the use of aortic measurements in early diagnosis and accurate prognosis of MFS patients. In order to do this, a method for extracting measurements across the entire length of the aorta from the segmentation result is needed. Also, the segmentation errors must be corrected to extract accurate measurements that represent the true aorta.

5.2 Old Method

The measurement extraction process was performed in the following manner described in [4].

1. The centerline was extracted using the algorithm described by Palagyi et al. [10] [11]. As the algorithm was developed for the pulmonary specific version, it was using only one anchor point. The algorithm was extended to two anchor points (start and end) to work with the aorta.
2. Vectors that denote the direction of the centerline were extracted by calculating the vectors between two adjacent centerline points.
3. The vectors were smoothed using an iterative smoothing algorithm based on the aortic diameter described as the Rolling Spheres approach in [4].
4. The planes perpendicular to the vectors were calculated.
5. The planes were used to transform the aorta into a straightened surface using the Affine Transform equation.
6. A 3D editing tool was developed to edit the points in the straightened surface.
7. The edited surface was back transformed to CC coordinates.

8. The contour points were extracted using the planes perpendicular to the vectors. The classes *vtkCutter* and *vtkSplineFilter* were used from the VTK toolkit.
9. The contour points were used to calculate measurements such as Cross Sectional Area (CSA), Eccentricity, Curvature and Centroid of the contour points. The volume between the two slices was also calculated. The application developed by Kyungmoo Lee for coronary artery analysis was utilized along with many Perl scripts to reformat the measurements to make it suitable for aorta analysis.

5.2.1 Problems

The above method sounds feasible but the implementation was extremely error prone, time consuming and the measurements were not believable. It consisted of the following problems:

1. The algorithm took about 40 minutes to extract the smoothed vectors in each phase using the Rolling Spheres approach. The implementation of this method was far more complicated than required.
2. The straightening of the aorta and back transforming to CC coordinates contributed to the errors in measurement.
3. There were many intermediate uses of Perl scripts so the complete process was not streamlined.
4. The measurements did not correspond with the clinical knowledge. The size of the aorta was getting bigger near the diaphragm for a normal subject as shown in Figure 5.1 on page 18.
5. There was no method to easily visualize the errors in each stage of the pipeline for each case.

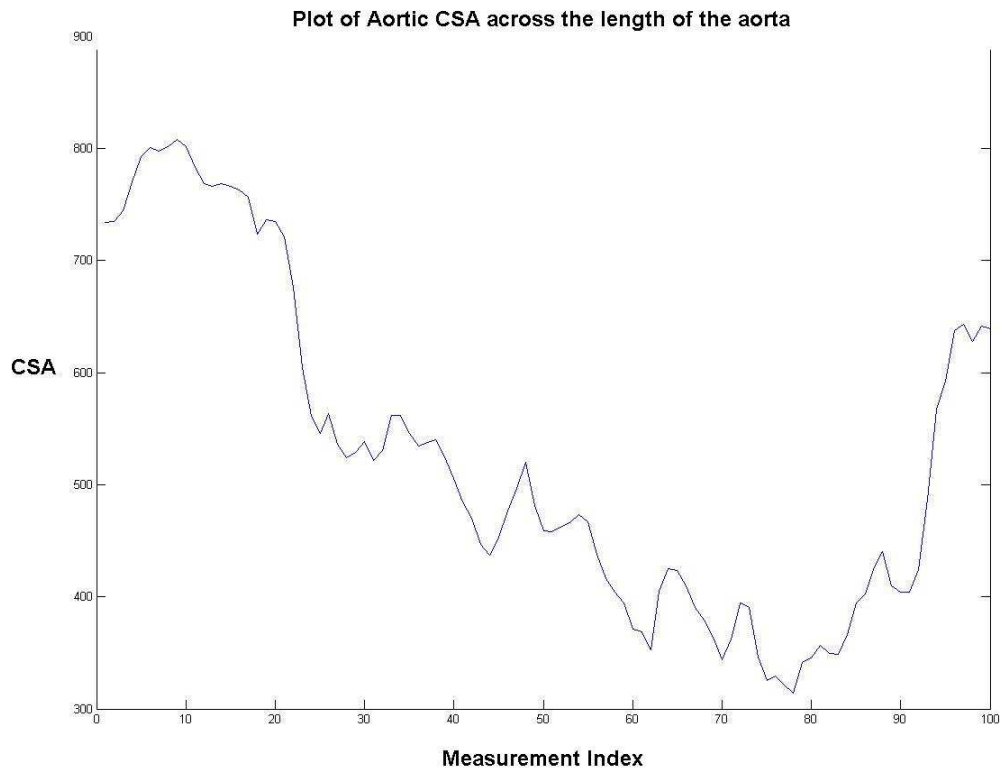


Figure 5.1: Cross Sectional Area (CSA) measurements in mm^2 across the length of the aorta in a normal subject for a single phase obtained using the old method. Note - The aorta is getting bigger near the diaphragm does not correlate with clinical knowledge

5.3 New Method

5.3.1 Overview

As the above method was faulty at multiple levels, a complete re-assessment was needed. A much simpler and methodical approach was taken that will enable us to identify the problems easily and correct for it. The following changes were enforced from a broad perspective:

1. The step of straightening the aorta from CC coordinates to a straightened surface for 3D editing and back transforming to CC coordinates after editing, was removed. Instead, editing was done in CC coordinates in a 2D interface. More

details about the GUI are explained in Section 5.3.9 on page 30.

2. VTK rendering was used to display the intermediate results in an interactive interface to validate them on a case-by-case basis. More details about this are explained in Section 5.3.9 on page 30.
3. The source code from the coronary artery analysis application was integrated along with the aorta analysis code so the need to use intermediate Perl scripts is eliminated.

Along with this, the details of the algorithms and the interface were also changed as explained below.

5.3.2 Volumetric Object Creation

The volumetric object was created by converting the segmentation image data into a VTK Polydata surface. The same sequence of filters described in [4] were used. It utilized the marching cubes algorithm to extract the volumetric surface and the surface was smoothed using a 3D low pass filter. The smoothing of the aorta affected the volume of the aorta as shown in Figure 5.2 on page 20. The value of 0.01 was chosen as the smoothing parameter of the smoothing filter as it provided the optimal visual result as shown in Figure 5.2 on page 20.

5.3.3 Centerline Extraction

The same methodology as described in [4] is used for extracting the centerline. The coding in the old method was more complicated than necessary and the excessive use of pointers could be a possible cause of memory leaks, so the entire code was rewritten. The centerline extraction is performed on the segmentation image data and it only provides the indices of the pixels that form a centerline in the image. This would correspond to the locations in an image with voxel size of $1mm^3$. The old method forced the segmentation image to contain a voxel size of $1mm^3$ to correlate with the

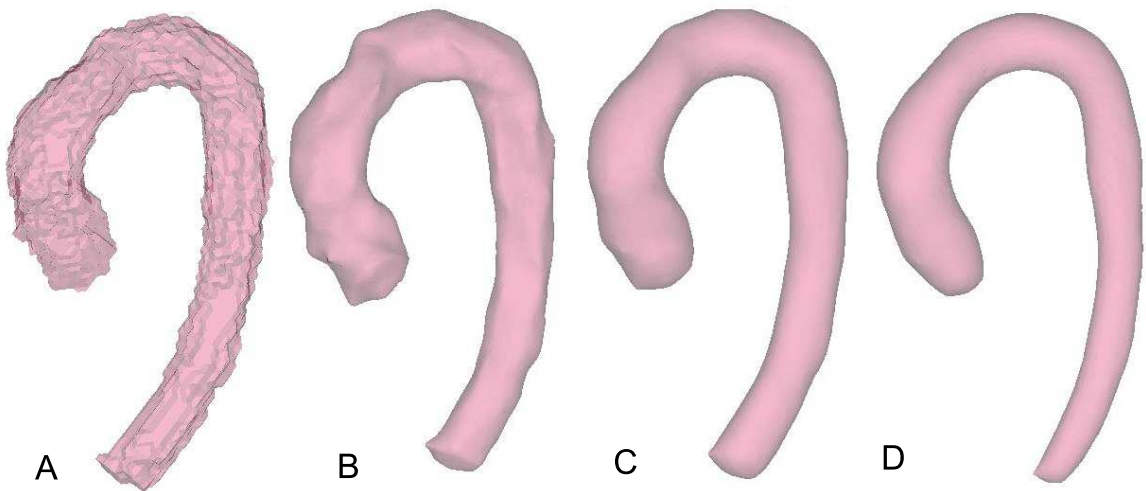


Figure 5.2: Aortic Volume Creation - Effect of Smoothing Parameter. A - No Smoothing, B - 0.1, C - 0.01, D - 0.0001

centerline extraction process but this step would produce incorrect measurements. An example of using the aortic volume scaled to its voxel size and the centerline without scaling is shown in Figure 5.3 on page 21. The new method corrected this error by scaling the centerline to suit the voxel size instead of forcing the image to have a voxel size of $1mm^3$. The extracted centerline was validated using the VTK interface as shown in Figure 5.4 on page 22.

5.3.4 Normal Vector Calculation

The normal vectors describe the plane to extract contour points at each measurement location. The normal vectors are obtained by calculating the vector between a centerline point and its neighbor. The normal vectors have to be smoothed in order to attain parallel contour point planes.

The old method performed the smoothing using an iterative vector averaging method described as the Rolling Spheres Approach in [4]. The premise is to smooth the vectors based on the radius of the aorta at that location as described in [4]. It consists of the following general steps:



Figure 5.3: Aortic volume scaled to real world coordinates and centerline in image coordinates. The image is scaled and translated in 3D with respect to the centerline but the 2D graphic does not show it clearly.

1. The contour points were extracted using the original vectors and the radius was obtained using the contour points.
2. The radius at each point was used to determine the smoothing window for that point
3. The above steps were performed 3 times as it was found that it reached a minima by the third iteration.

The new method consists of smoothing each vector based on 3 neighbors on either side. This process worked well in all the tested cases given that the aorta was smooth

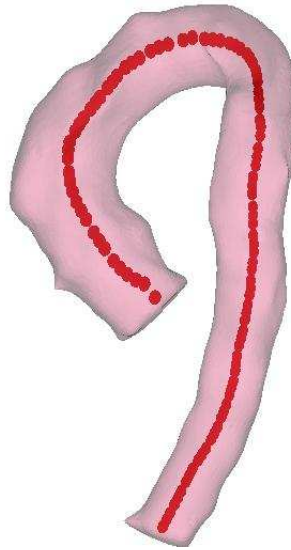


Figure 5.4: Aortic Volume along with the centerline.

and the start and end points were placed correctly. It was almost instantaneous. The reasons it worked and a discussion of the previous method are explained below.

- A small directional change in the centerline extraction process creates vectors that produce massively overlapping planes. These variational changes were not available in all the vectors. They were intermittently present among the centerline points.
- Smoothing drastically changes the direction of the vectors that were outside the trends of its neighbors but it does not affect the vectors that are following a general trend. The smoothing window is only essential to capture the global direction of the centerline so a sufficiently large smoothing window will suffice.

The validation was performed by visualizing the planes cutting through the aorta as shown in Figure 5.5 on page 23.

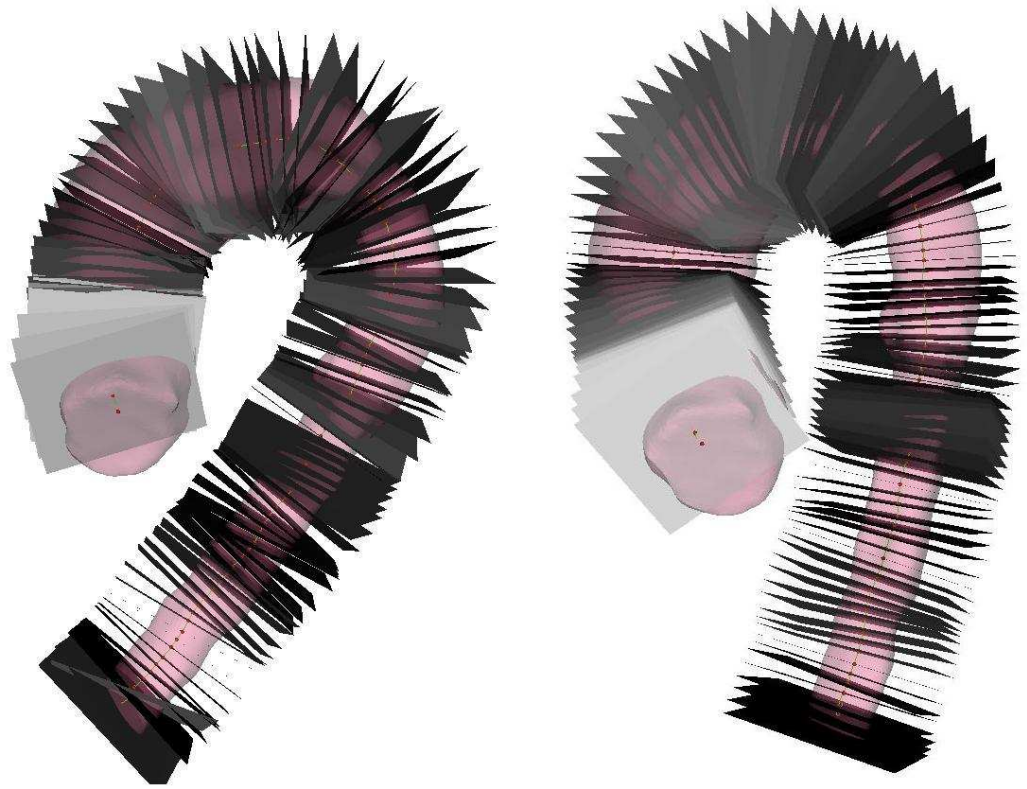


Figure 5.5: Aortic volume along with the cross section planes used to extract the contour points. Left - non smoothed planes, Right - Smoothed Planes.

5.3.5 Contour Points Extraction

The contour points were extracted similar to the old method using the *vtkCutter* algorithm and extracting equidistant points (100) from the *vtkSplineFilter* algorithm. The *vtkCutter* would cut through more than one surface in the aorta in certain regions. In these cases, the number of points that were extracted were scaled by the number of surface cuts. The previous method only accounted for two surface cuts, however, more than two cuts were made in certain aortas with mis-segmentations. Hence, this method was rewritten to account for any number of cuts made by *vtkCutter*.

5.3.6 Contour Points Ordering

The extracted points must be ordered to produce accurate measurements, i.e. each point in an array must be the closest point to the next one in the array (Slice Ordered). Similarly, the index of each point in the array of points in one slice should have the same index to the closest point in the next slice (Volume Ordered).

The previous method used the distance to the centerline as a metric to separate the points that made multiple cuts across the aorta. However, this removes the ordering of points produced by the *vtkCutter* algorithm. Hence, each point needed to be checked with all the other points in a slice to Slice Order the points. Similarly the points must be re-ordered by checking the index and distance between the points in neighboring slices. This was a time consuming process.

The new method utilized the inherent Slice Ordering of the *vtkCutter* class and stored only the set of Slice Ordered points that were closest to the centerline point. This was done by calculating the distance to the centerline of the starting point of each cut and storing only the set of points whose starting point is closest to the centerline point. This process was much more efficient and accurate.

Volume Ordering was performed the following way:

1. The start point of each slice was compared to each point in the next slice. The points in the next slice were re-ordered so the point closest to the starting point of the previous slice would have the same index. This process can be imagined as twisting the points in the next slice to align the start points of both slices.
2. The above method will fail to produce correct results if the points in each slice were ordered in both clockwise and counter-clockwise directions. This was corrected by checking the another index point (6) of one slice to the same index point of the next slice and number of points - index point of the next slice. If the latter had a closer distance to the examining point then the points are arranged in opposite directions and the ordering was corrected.

The ordering of volume was analyzed by drawing lines between the contour point indices in a slice and contour point indices between two slices. The complete aorta was validated using a small number of contour and centerline points and using a larger number of points in a single slice as shown in Figure 5.6 on page 25.

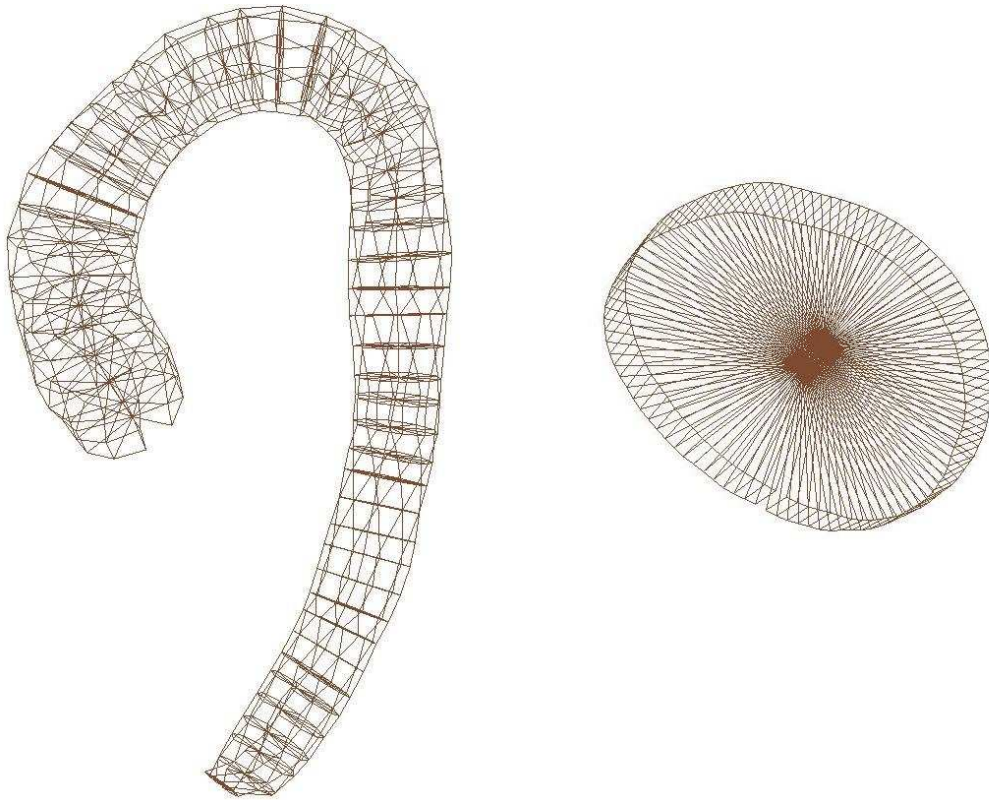


Figure 5.6: volumetric cubes connecting the contour points of the aorta. Left - 10 contour points per slice connected through the whole aorta. Right - 100 contour points for a single slice.

5.3.7 Measurement Calculation

The initial source code for measurement calculation was written by Kyungmoo Lee for the coronary artery analysis application. The previous method interfaced with the application by providing the contour points as an input and reformatting

the output measurements from the application to suit aorta analysis using many Perl scripts. This system would be unusable by a clinician.

The new method integrated the measurement calculation along with the aorta analysis code with minor modifications. The following measurements were calculated using the ordered contour points:

- Average Diameter - The average of all the diameters extracted from the contour points.
- Centroid - The centroid of the contour points
- Cross Sectional Area - The cross sectional area was calculated by creating triangles between the consecutive contour points and the centroid. The sum of the area of all the triangles in a slice is the cross sectional area of the slice.
- The volume between two slices is calculated using the polytope method described in [12].
- Eccentricity - Eccentricity of a slice is the ratio of the maximum diameter and minimum diameter of the slice.
- Curvature - The curvature in the X, Y and Z direction are calculated as prescribed in [13].

5.3.8 Measurement Validation

There are three possible sources of error in extracting the contour measurements.

1. The contour points might not be distributed and aligned properly across the entire aorta.
2. The contour points might not be ordered which will produce incorrect measurements.

3. The measurement calculation process might be wrong or have a large source of error.

The following validation techniques were used for identifying the sources of error:

1. The contour points were displayed along with the aortic segmentation in an interactive 3D visualization interface using VTK. The points were also displayed as a spline as shown in Figure 5.8 on page 30. The spline was drawn between consecutive indices hence any mistakes in ordering could be seen by visualizing the splines. Also, the spline was not drawn between the last point and first point in the contour points array. This allowed for visualizing the Volume Ordering of the points as it created a seam like appearance as shown in Figure 5.8 on page 30. These visualization capabilities were provided in a user interface as explained in Section 5.3.9 on page 30 to identify any mistakes in a case-by-case basis.
2. The errors in measurement calculation were validated by creating a straight cylinder of ordered contour points in floating point space. The measurements used were a diameter of 10mm and contour interval of 2mm. A figure of the cylinder is provided in 5.7 on page 28. The calculated values and the measurement errors are given in table 5.1 on page 29.
3. The complete measurement extraction process from a binary segmentation image was validated using aortic phantoms with varying diameters. The phantom was created using *itkSpatialObjects* classes in the ITK toolkit to have an approximate shape of the aorta. The start and end points were identified manually and the centerline, contour points and measurements were extracted using the new method. A figure of the binary volume, centerline and extracted contours is shown in Figure 5.8 on page 30. The plot of the measurements for a binary phantom of 40mm diameter is provided in Figure 5.9 on page 31. The mean and

standard of deviation of the measurement errors for Diameter across the entire length for varying diameters are given in table 5.2 on page 29. The mean and standard deviation of the phantom measurements show that there is minimal error of upto 1mm for the entire measurement calculation process for an aortic shaped phantom in the subject range. In most cases, the measurements are under-estimated. This may be because the volume was smoothed before the measurements were extracted.

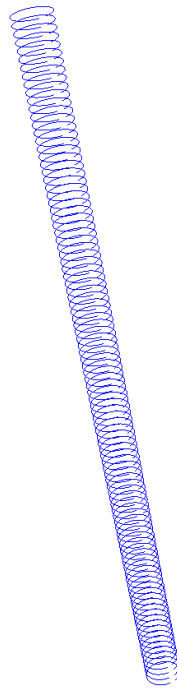


Figure 5.7: Straight Phantom Cylinder Created in Floating Point Space. Diameter = 10mm, Interval = 2mm.

Table 5.1: Measurements and Errors For Each Slice Of Straight Cyclindrical Phantom Of Diameter = 10mm, Interval = 2mm

Label	Diameter (mm)	CSA (mm ²)	Volume (mm ³)	C (X)	C (Y)	C (Z)
Measurement	9.99	78.42	156.82	0	0	0
Error	0.01	0.15	0.32	0	0	0

^a C - Curvature

Table 5.2: Measurement Error For Aortic Binary Phantom With Various Diameters

Diameter(mm)	mean error (mm)	std error (mm)
10	0.91	0.07
20	0.87	0.07
30	0.75	0.12
40	0.62	0.22
50	0.46	0.33
60	0.25	0.49

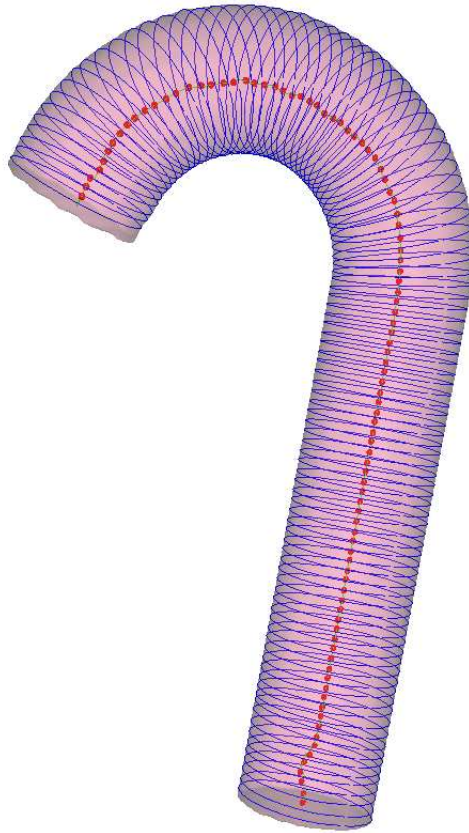


Figure 5.8: Binary Phantom of 40mm diameter along with the contour points shown as splines. Note the centerline extraction error near the diaphragm area fixed the smoothing of normals.

5.3.9 User Interface

While the above method has worked robustly in the aortic phantom, it is imperative to check the contour extraction process and measurements in a case-by-case basis for a wide variety of patient and normal aortic segmentations. Also, the segmentations might have some errors that must be corrected to extract accurate aortic measurements.

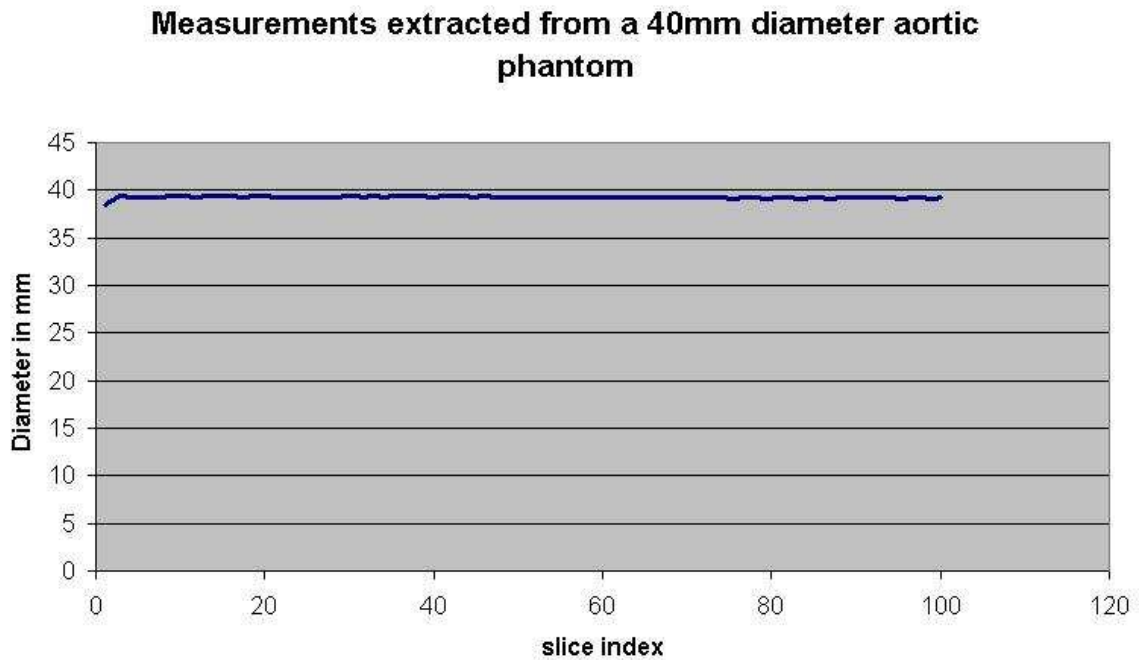


Figure 5.9: Diameter of the Binary Phantom.

5.3.9.1 Old Method

The old method provided an interface to view the original image, the aortic original image in a straightened view and the segmentation results as contours in the straightened image. The contour has 100 points with 10 anchor points at equal intervals that can be moved. The user can edit the contours using a 3D editing algorithm. Moving an anchor point will move other anchor points three-dimensionally as prescribed by a Gaussian equation. The intermediate points between the moved anchor points were re-oriented based on the Catmull-Rom spline equation. A point wise correlation between the original CC image and straightened image was used by clicking on the straightened image and analyzing its position on the CC image. The corrected points were then back transformed to CC coordinates to extract the measurements.

5.3.9.2 New Method

The new method consisted of an interface with the following features:

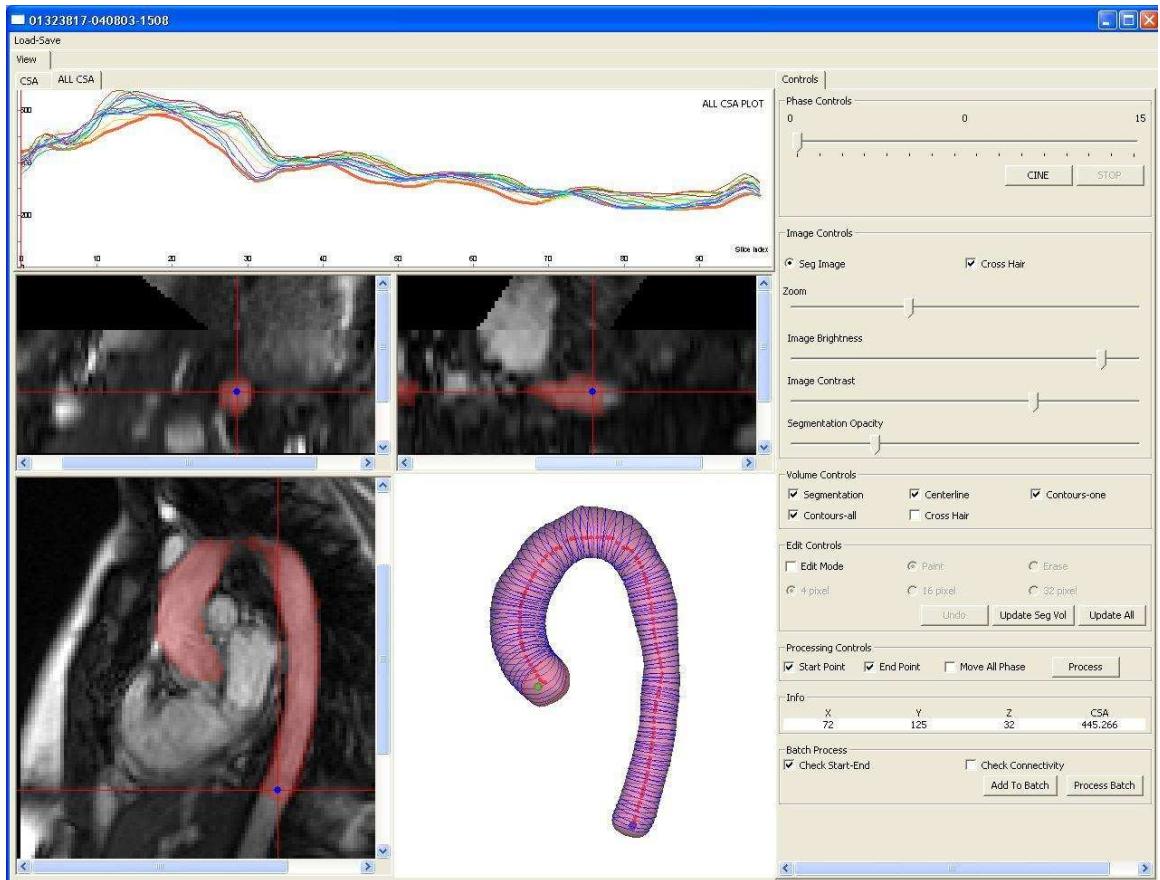


Figure 5.10: Aortic Analysis Viewer.

- The original CC image is displayed along with the segmentation image as an overlay on the original image. The overlay opacity of the segmentation image can be changed to account for the user needs. The segmentation image is also displayed in an interactive 3D view with rotating, zooming and panning capabilities.
- If the segmentation image is processed, other tools are available as well:
 - All the extracted contours are displayed using the **all contour** tool in the interactive 3D interface.
 - The CSA measurement curve is displayed in a separate graph.

- Each CSA measurement can be correlated with its respective contour using the **one contour** tool.
- The centerline is displayed in an interactive 3D interface.
- All the 3D visualization tools can be viewed separately or together.
- If the segmentation is not processed, the following tools are available:
 - A point wise correlation between the 2D interface and 3D interface is provided using the **Cross Hair** tool.
 - The **Start Pt** tool displays the starting point of the centerline in the 2D and 3D interface. It can be dragged and moved in the 2D interface.
 - The **End pt** tool displays the ending point of the centerline in the 2D and 3D interface. It can be dragged and moved in the 2D interface.
 - The whole case can be processed by clicking the **Process** button. A warning is given and the processing stops if the start and end points are not within the segmentation image for any specific phase. More details on the error identification process is provided in
- If the segmentation needs to be edited, the following tools are available:
 - A paint brush of different sizes can be used to add segmentation pixels or erase segmentation pixels to the original image in the 2D interface.
 - The **Update Vol** tool updates the edited aortas in the 3D interface.
 - The **Update All** tool updates the edited aortas, recalculates the contours and measurements and displays the new contours and measurements. A warning is given and the processing stops if the start and end points are not within the segmentation image for any specific phase that is being updated.

- The editing, updating and visualization can be performed repeatedly to attain the desired result.
- Multiple unprocessed cases can be processed as a batch using the **Add To Batch** and **Process Batch** tool.

5.3.9.3 Error Identification

The centerline extraction process requires a single connected object without any holes to identify the centerline. Hence, the holes or extra objects created during the editing process should be identified and corrected before further processing. They were identified in the following ways:

1. The number of objects in the 3D image was identified in the following manner: Connected components were identified using the *itkConnectedComponentImageFilter* and the components were relabeled using the *itkRelabelComponentImageFilter*. Then the number of labels in the relabeled image were counted. An application error was sent out if there was more than one object.
2. The holes in an object were filled in the following manner: First, the external region to the object was identified using the *itkConnectedThresholdImageFilter* using the first point in the image as the seed point (Assumption: The first point does not contain the object). Then an OR operation was performed between the external region and segmentation object. These operations separate the holes from the external region and segmentation object allowing the identification of the hole voxels. The hole voxels are filled as the segmentation image.

5.3.9.4 Benefits

The user interface has the following benefits:

- Any discrepancy in the aortic segmentation shape can be easily seen in the 3D interface. Also, the inconsistencies in terms of its movement in 4D can also be

seen using the **Cine** tool. The cause of the disparity in the 3D interface can be identified by correlating it with the 2D image using the point wise correlation feature. Any needed edits can be performed using the **Edit** tools.

- Any discordance in the shape of the CSA measurements can be correlated with its respective contour orientation in the 3D interface. This tool may provide more insight into the shape of the aorta or it may lead to diagnosis about the errors in the segmentation process.

CHAPTER 6

MEASUREMENT ANALYSIS

The above tools allow a clinical user to segment the aorta and extract the measurements from LVOT and CC DICOM images. However, the exact clinical benefits of these measurements have not yet been analyzed. Various 3D and 4D geometric features can be calculated from the basic set of measurements explained in Sub-Section 5.3.7 on Page 25 and their utility in identifying the differences between normal subjects and patients can be examined. Also, the prognostic capability for patients can be assessed using these new features. More information on this is provided below.

6.1 Subject Information

Measurements for 152 aortic scans were extracted using the combination of the old and new method. Most of the scans were merged using the old method of merging. About three-fourth of the scans were segmented using the old method and the rest were segmented using the new method. All of the scans were analyzed and corrected using the new method. The analysis and correction was performed within a month using the new analysis software.

There were 78 scans for 32 normal subjects and 74 scans for 38 patients. The distribution of scans is given in Table 6.1 on Page 36.

Table 6.1: Scan Distribution

Heading	Normal Subjects	Patients
Number Of Subjects	32	37
Total Scans	78	73
Subjects with 1 scan	8	12
Subjects with 2 scans	10	17
Subjects with 3 scans	8	6
Subjects with 4 scans	4	2
Subjects with 5 scans	2	1

6.2 Scan Analysis

6.2.1 Measurement Database

The above application allowed the processing of a single scan but the analysis required an aggregation of all the scans and proper sorting based on patient ID and scan date. Hence, a matlab script was used to recursively identify all the scan information from the parent folder and sort them in a hierarchical datastructure based on patient ID. Each patient ID consisted of many scans with their respective dates and measurement information. The datastructures were stored as a matlab datastructure file so it can be saved and reloaded easily facilitating multiple experiments with minimal overhead. A separate datastructure for normal subjects and patients were used.

6.2.2 Feature Extraction

The following 3D and 4D geometric features were extracted from basic set measurements calculated from the contour points as explained in Sub-Section 5.3.7 on Page 25.

- Max CSA and Min CSA - The maximum and minimum cross sectional area(CSA) across all the phases for the entire thoracic aorta.
- Max Change in CSA - The difference between Max CSA and Min CSA per location for the entire aorta. This is a measure of distensibility of the aorta.
- Percent Change in CSA - The percentage of Max Change in CSA as compared with Min CSA per location for the entire thoracic aorta. This is a measure of the relative distensibility of the aorta in comparison to its original size.
- Rate of Change in CSA - The difference in CSA across consecutive phases were calculated per location for the entire thoracic aorta. Then the maximum of the absolute values of the differences were obtained and divided by the time interval

between two phases. This is a measure of the speed of aortic distension.

- Eccentricity - The maximum eccentricity across all phases per location for the entire thoracic aorta. Eccentricity is defined as the Maximum Diameter over the Minimum Diameter at each location in the aorta. An eccentricity of 1 denotes a circle and the shape becomes more elliptical as the value increases.
- Centroid Movement - The maximum distance moved by a centroid point per location through the entire thoracic aorta.
- Curvature - The maximum magnitude of the curvature across all phases per location through the entire thoracic aorta.
- Curvature Change - The maximum change in curvature across all phases per location for the entire thoracic aorta.

6.2.3 Feature Plots

The Mean and Standard Deviation for the features were plotted across the entire aorta between normal subjects and patients to identify their differences. Mean and Standard Deviation was calculated between 34 Normal Subjects and 38 patients. If a subject had more than one scan, the average of the scan measurements were considered. Also, the scans in each patient were plotted along with the 5th and 95th percentile measurements among all normal subject scans to compare the prognostic capability of these new features. Some interesting observations noted during this process are shown below.

- The Mean and Standard Deviation plots for Max CSA in Figure 6.1 show that the mean dilation is greater for patients across the entire aorta, though there is a clearer separation in the proximal region of the aorta. In certain cases, the proximal regions of the aorta are within the normal range but dilation is seen in the distal region as shown in Figure 6.3. An interesting reduction in the

CSA after surgery is also shown in a Figure 6.4. An example of a patient with 5 consecutive scans is also shown to display the reproducibility and possible prognostic capability of measurements across the entire aorta in Figure 6.2.

- The Centroid Movement for patients in the proximal locations (Slice 1 - 20) of the aorta are lower than that of normal subjects while it is similar to the normal subjects in the distal regions as shown in Figure 6.5. The movement in the distal locations is very minimal (About 2 mm) hence no differentiation is expected. But the proximal regions are not responding to blood pumping effect in patients as much as normal subjects. This can be an important 4D feature that allows in early diagnosis of Marfan patients. Centroid movement is also consistently lower in many patients and are consistent between multiple scans for a patient as shown in Figure 6.6.
- The Max Change in CSA plot shows that patients are distending more than normal subjects on an average as shown in Figure 6.7. However, the Percent Change in CSA plot shows that the relative distensibility of patients is lower than the normal subjects on an average as shown in Figure 6.8. Hence, absolute distensibility might not be a good indicator since it accounts for the size of the aorta. Both plots have a large area of overlap between normal subjects and patients so more studies should be performed to identify the validity of these features. It is important to note that change in CSA is sensitive to image resolution, segmentation efficacy and contour location between different phases. This might also be the cause of overlap between normal subjects and patients in the distensibility plots.
- The Curvature and Curvature Change are not different between normal subjects and patients as shown in Figures 6.9 and 6.10. The increased curvature at the the locations between the 30th and 40th index corresponds with aortic arch in

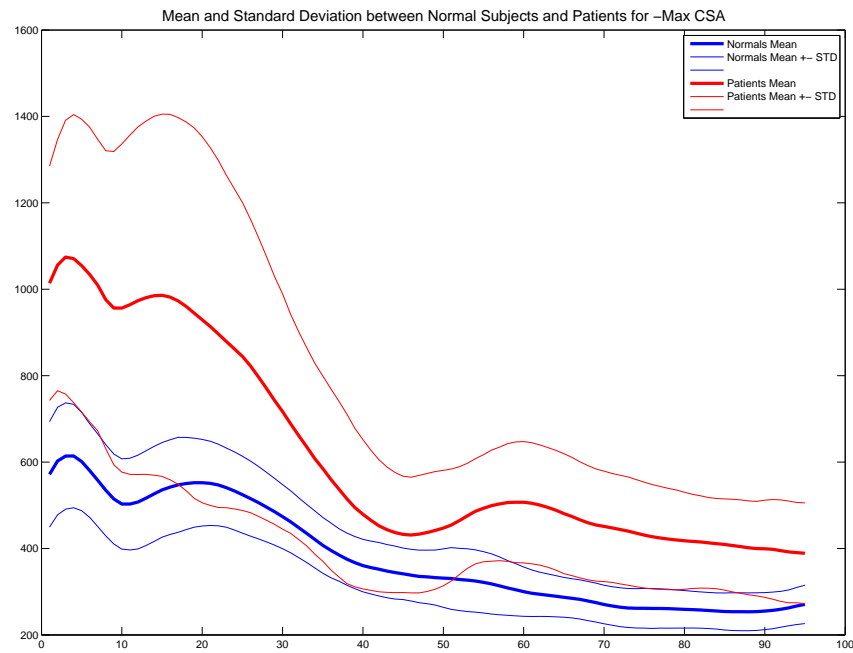


Figure 6.1: Max CSA distribution between normal subjects and patients

a few tested cases.

- The mean Eccentricity is slightly higher for patients than for normal subjects as shown in Figure 6.11, though there is a significant overlap. This is not consistent in all the patients but significantly present in some. Eccentricity is also sensitive to image resolution and segmentation accuracy.

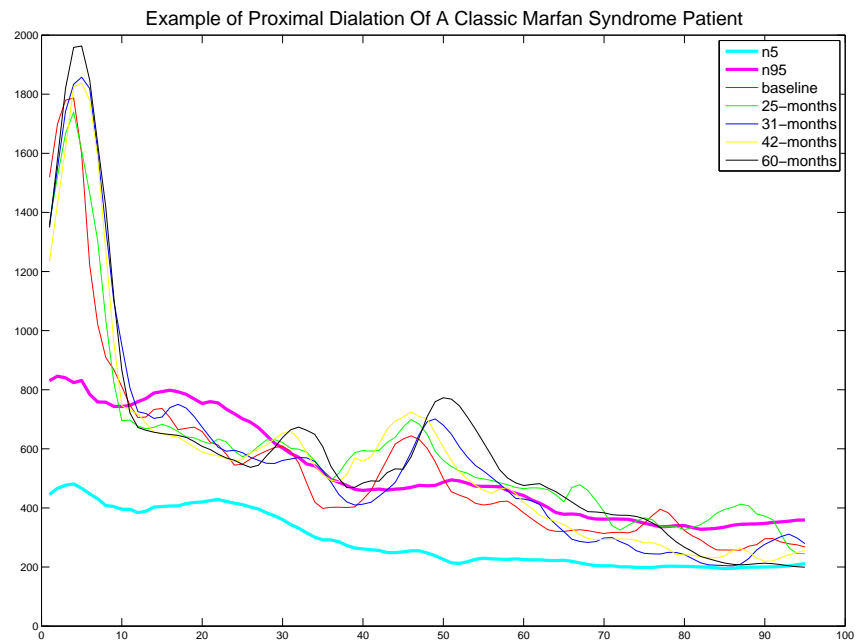


Figure 6.2: Max CSA for patient with 5 consecutive scans

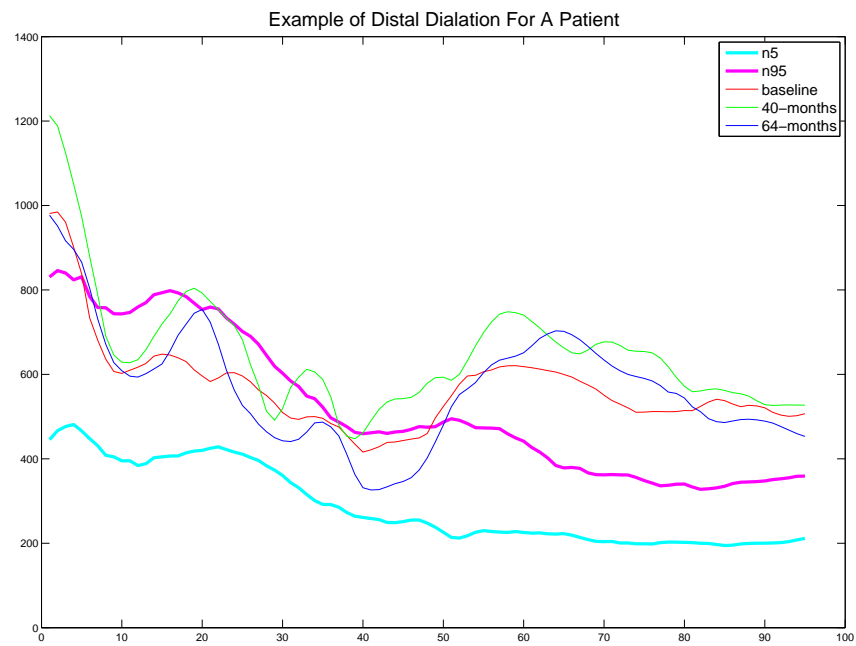


Figure 6.3: Patient with distal dialation in sequential scans

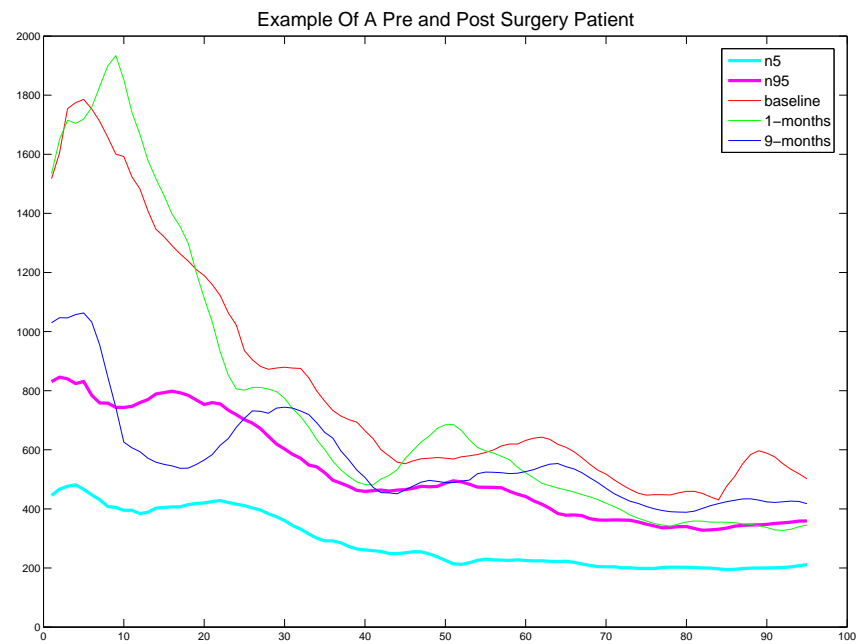


Figure 6.4: Pre and post Surgery CSA

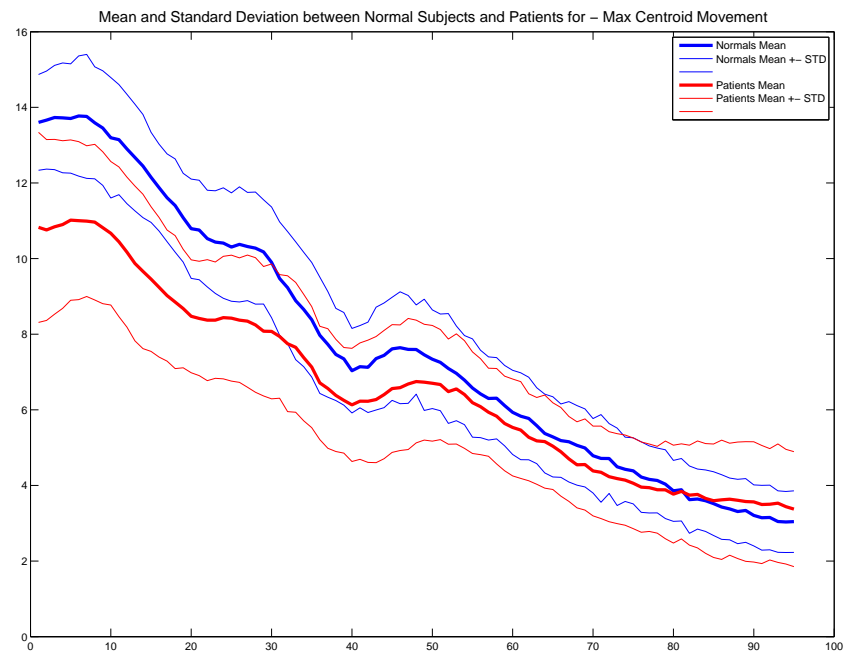


Figure 6.5: Centroid Movement plot between normals and patients

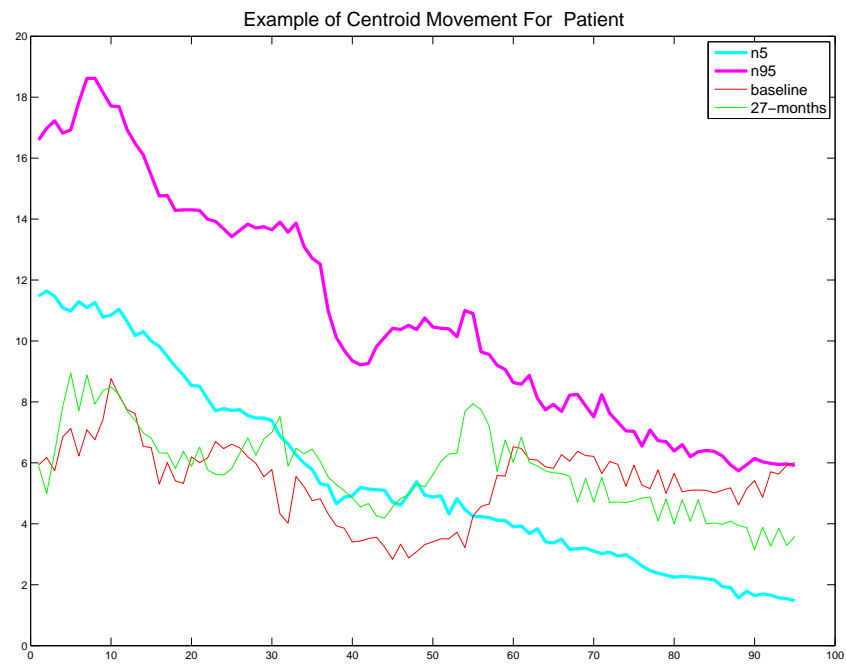


Figure 6.6: Centroid Movement Scan for a patient with sequential scans

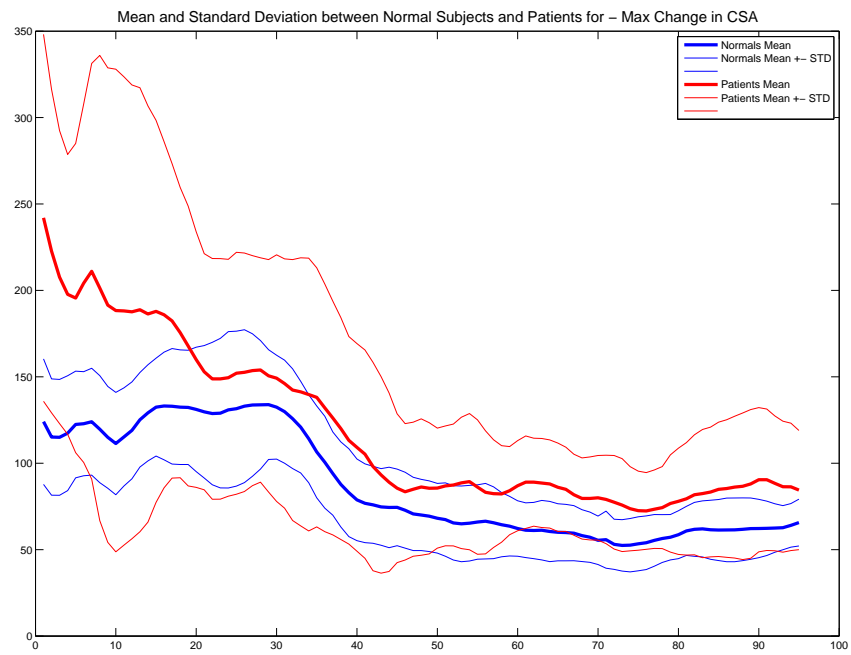


Figure 6.7: Distensibility distribution between normal subjects and patients

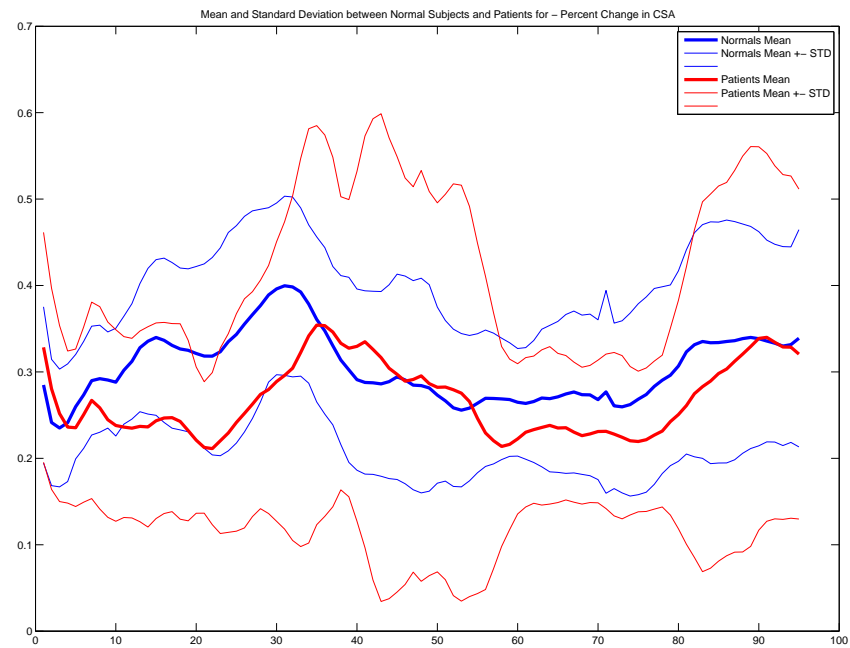


Figure 6.8: Distensibility distribution between normal subjects and patients

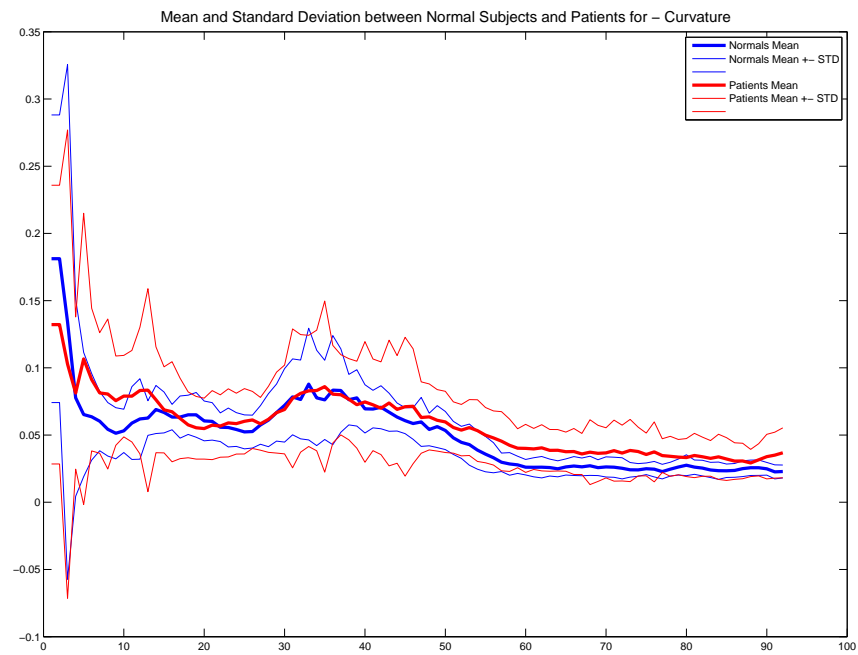


Figure 6.9: Curvature distribution between normal subjects and patients

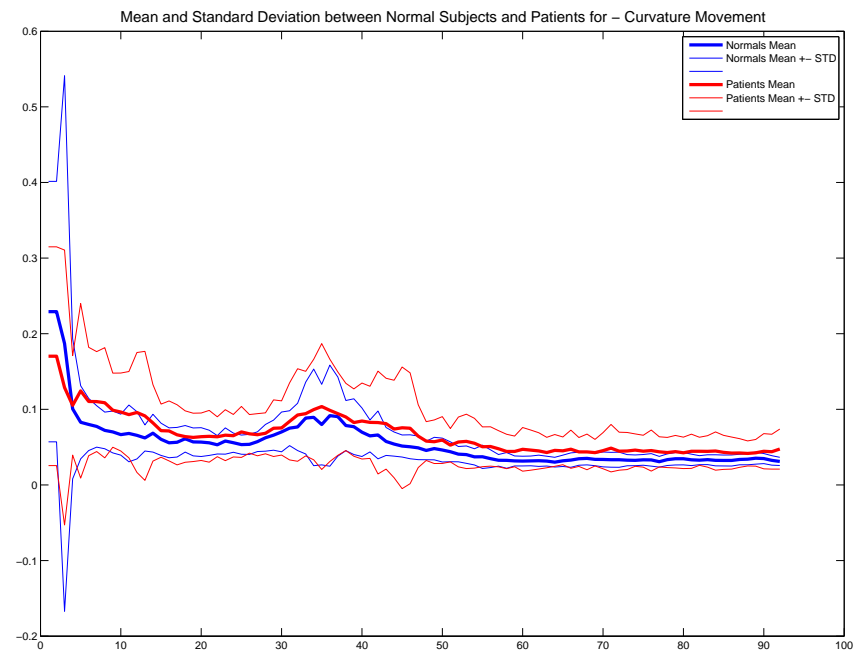


Figure 6.10: Curvature Change between normal subjects and patients

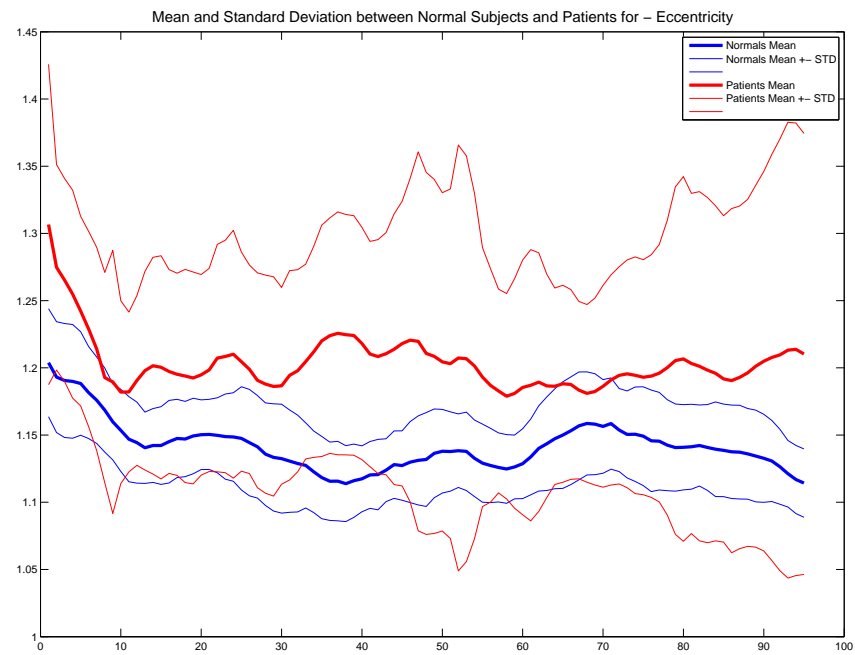


Figure 6.11: Eccentricity between normal subjects and patients

CHAPTER 7 CONCLUSION

7.1 Conclusion

- A connected set of applications was created to extract multiple quantitative measurements from LVOT and CC CINE Aortic MRI images by integrating and altering the existing research algorithms developed for this purpose.
- The utility of these applications combined with the research algorithms are demonstrated by extracting measurements on 151 scans from DICOM images.
- The robustness of the measurements are demonstrated through its consistency between sequential scans for a subject.
- The benefits of the measurements are also analyzed and some interesting observations are shown.

7.2 Future Work

- The developed technology provides the basis to process multiple scans with minimal user effort. So the project is easily expandable to test multiple hundreds of scans with some extra development. The connected applications should be integrated into a single intelligent interface which tracks the processing of a scan from DICOM to measurement extraction and allows the user to edit the intermediate results at various stages for quick and efficient processing for a wide dataset. Also, a backend database infrastructure should be developed so multiple scan measurements and image data for a patient are stored and displayed when necessary. A client-server model can also be incorporated for a large multi-location study.
- At first pass, the observations demonstrate the usefulness of these measurements. However, the measurements given above have to be thoroughly analyzed with rigorous statistical testing for credible publications.

- The 3D and 4D features display differentiation capability for different features between patients and normal subjects. However, all of them have an overlapping region. Hence, a combination of features can be used to classify the patients and normal subjects in higher dimensional space using pattern recognition techniques. The optimal combination of features can be extracted via a bottom-up approach using hypothesis testing or using a top-down approach using techniques such as principal component analysis and linear discriminant analysis. Then classification can be performed with the wide array of classifiers available.

REFERENCES

- [1] “The National Marfan Foundation,” <http://www.marfan.org/>, Nov 2008.
- [2] R. Pyeritz, *Principles and Practises of Medical Genetics*. New York: Churchill Livingstone, 1997.
- [3] D. Silverman, K. Burton, J. Gray, M. Bosner, N. Kouchoukos, M. Roman, M. Boxer, R. Devereux, and P. Tsipouras, “Life expectancy in marfan syndrome,” *American Journal Of Cardiology*, no. 75, pp. 157 – 160, 1995.
- [4] M. Thomas, “Extraction of Quantitative Measures Of The Aorta From Four Dimensional Segmentation of MR data,” Master’s thesis, University Of Iowa, 2008.
- [5] H. Gray, *Anatomy of the human body*. Philadelphia: Lea and Febiger, 1918, bartleby.com 2000 www.bartleby.com/107.
- [6] M. General Hospital, “Aortic dissection,” <http://www.massgeneral.org/>, Nov 2008.
- [7] M. Roman, R. Devereux, R. Kramer-Fox, and J. O’Loughlin, “Two-dimensional Echocardiographic aorticroot dimensions in normal children and adults,” *American Journal of Cardiology*, no. 64, pp. 507–512, 1989.
- [8] H. Zhang, “Segmentation and Computer Aided Diagnosis of Cardiac MR Images using 4-D Active Appearance Models,” Ph.D. dissertation, University Of Iowa, 2007.
- [9] F. Zhao, “Congenital Aortic Disease: 4D Magnetic Resonance Segmentation and Quantitative Analysis,” Ph.D. dissertation, University Of Iowa, 2007.
- [10] K. Palagyi, “Quantitative Analysis of Pulmonary Airway Tree Structures,” *Computers in Biology and Medicine*, no. 36, pp. 974 – 996, 2006.
- [11] K. Palagyi, E. Sorantin, E. Balogh, A. Kuba, C. Halmai, B. Erdohelyi, and K. Hausegger, “A Sequential 3D Thinning Algorithm and its Medical Applications,” *IPMI*, no. 2082, pp. 409 – 416, 2001.
- [12] R. Medina, A. Wahle, M. Olszewski, and M. Sonka, “Three Methods for Accurate Quantification of Plaque Volume in Coronary Arteries,” *The International Journal of Cardiovascular Imaging*, no. 19, pp. 301 – 311, 2003.

- [13] ———, “Curvature And Torsion Estimation for Coronary-Artery Motion Analysis,” *SPIE Proceedings*, no. 5369, 2004.